iScience, Volume *26*

Supplemental information

KMT2D suppresses Sonic hedgehog-driven medulloblastoma progression and metastasis

Reeti Mayur Sanghrajka, Richard Koche, Hector Medrano, Salsabiel El Nagar, Daniel N. Stephen, Zhimin Lao, N. Sumru Bayin, Kai Ge, and Alexandra L. Joyner

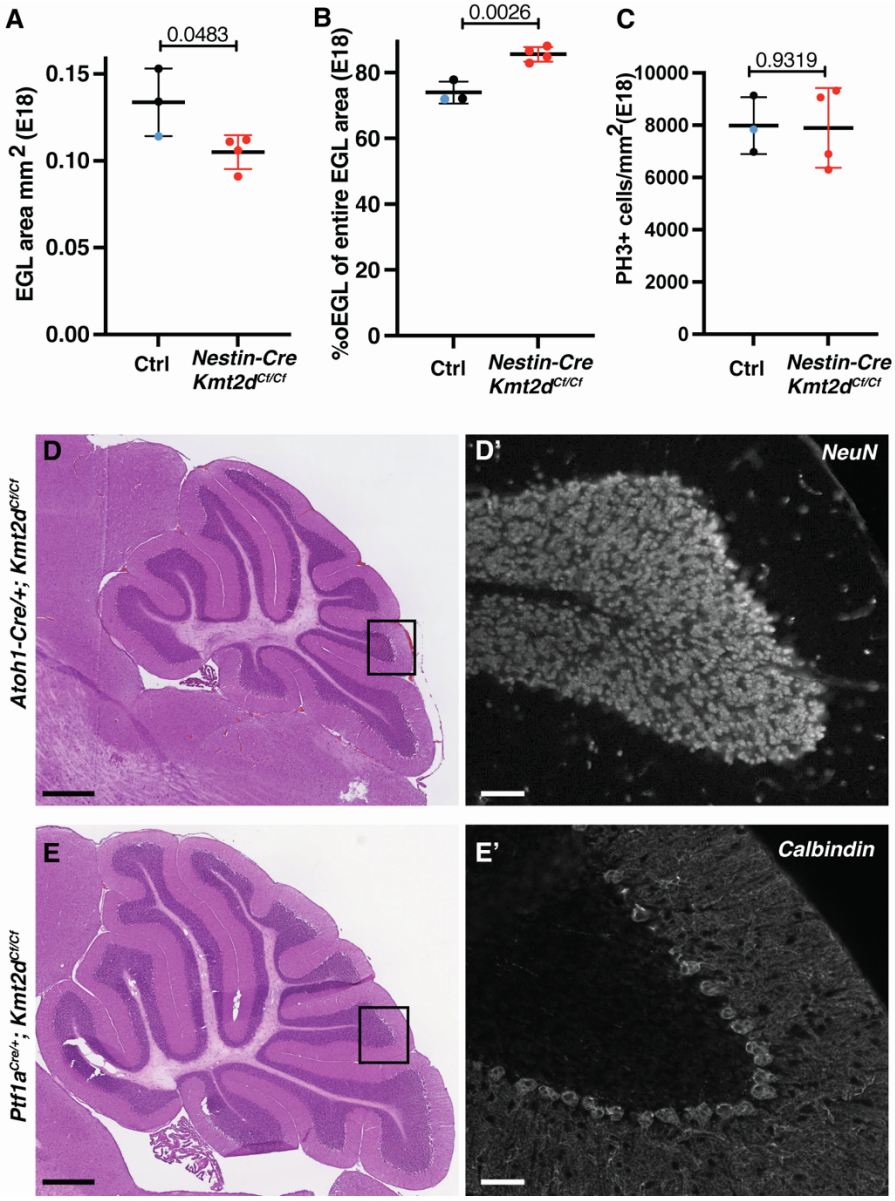

Figure S1: *Kmt2d*$^{Cf/Cf}$ conditional mutants have a reduced EGL at E18.5 but express cell type-specific differentiation markers at P21. Related to Figure 1.

(A-C) Cerebellar quantifications in E18.5 control *Kmt2d*$^{Cf/+}$ and *Kmt2d*$^{Cf/Cf}$ (black dots) or *Nes-Cre/+; Kmt2d*$^{Cf/+}$ (blue) embryos compared to *Nestin-Cre/+; Kmt2d*$^{Cf/Cf}$ (red) mutants. Cerebellar EGL area (A), the area of the outer EGL (P27-negative layer) as a percentage of the entire DAPI+ EGL area (B) and proliferation index, measured as the density of PH3+ cells in the outer EGL (C).

(D) Image of an H&E-stained sagittal section from a *Atoh1-Cre/+; Kmt2d*$^{Cf/Cf}$ adult animal (>P30). Scale bar = 500μm.

(D') Fluorescent image of NeuN expression in granule neurons in the IGL of a *Atoh1-Cre/+; Kmt2d*$^{Cf/Cf}$ mouse (*Scale bar = 50μm*).

(E) Image of an H&E -tained mid-sagittal section from a *Ptf1a*^{Cre}*/+; Kmt2d*$^{Cf/Cf}$ adult animal (>P30). Scale bar = 500μm.

(E') Fluorescent image of Calbindin expression in Purkinje Cells of a *Ptf1a*$^{Cre/+}$*; Kmt2d*$^{Cf/Cf}$ adult animal. Scale bar = 50μm.

Statistical significance was determined using an unpaired t-test. Error bars: S.D.

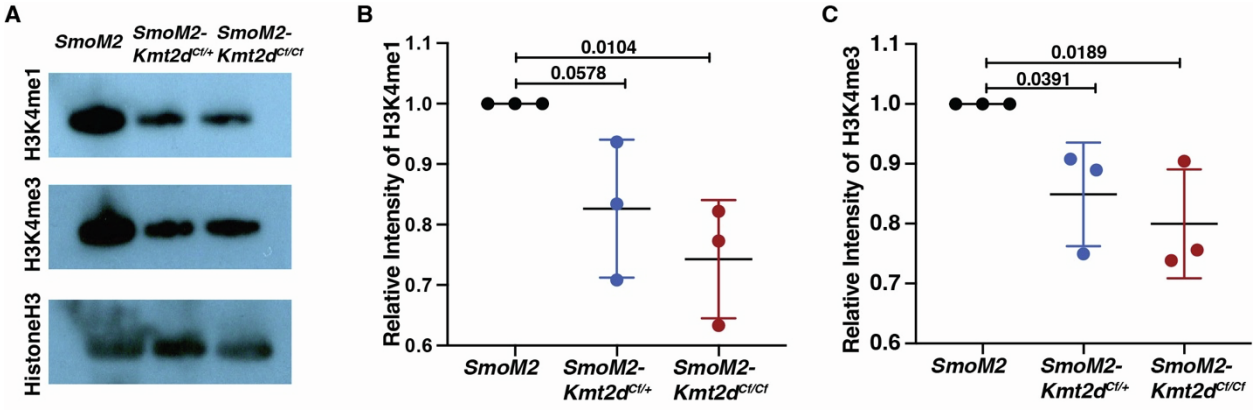

Figure S2: Heterozygous and homozygous loss of *Kmt2d* in the *SmoM2-Kmt2d^{Cf}* tumor models reduces histone 3 K4me1/3. Related to Figure 2.

(A) Representative western blot of H3K4 methylation.

(B, C) Quantification of the relative signal intensity of H3K4me1 (B) and H3K4me3 (C) from western blots (n=3). Statistical significance was determined using an unpaired t-test comparing *Kmt2d* wildtype tumors to each of the *Kmt2d* mutants as indicated. Error bars: S.D.

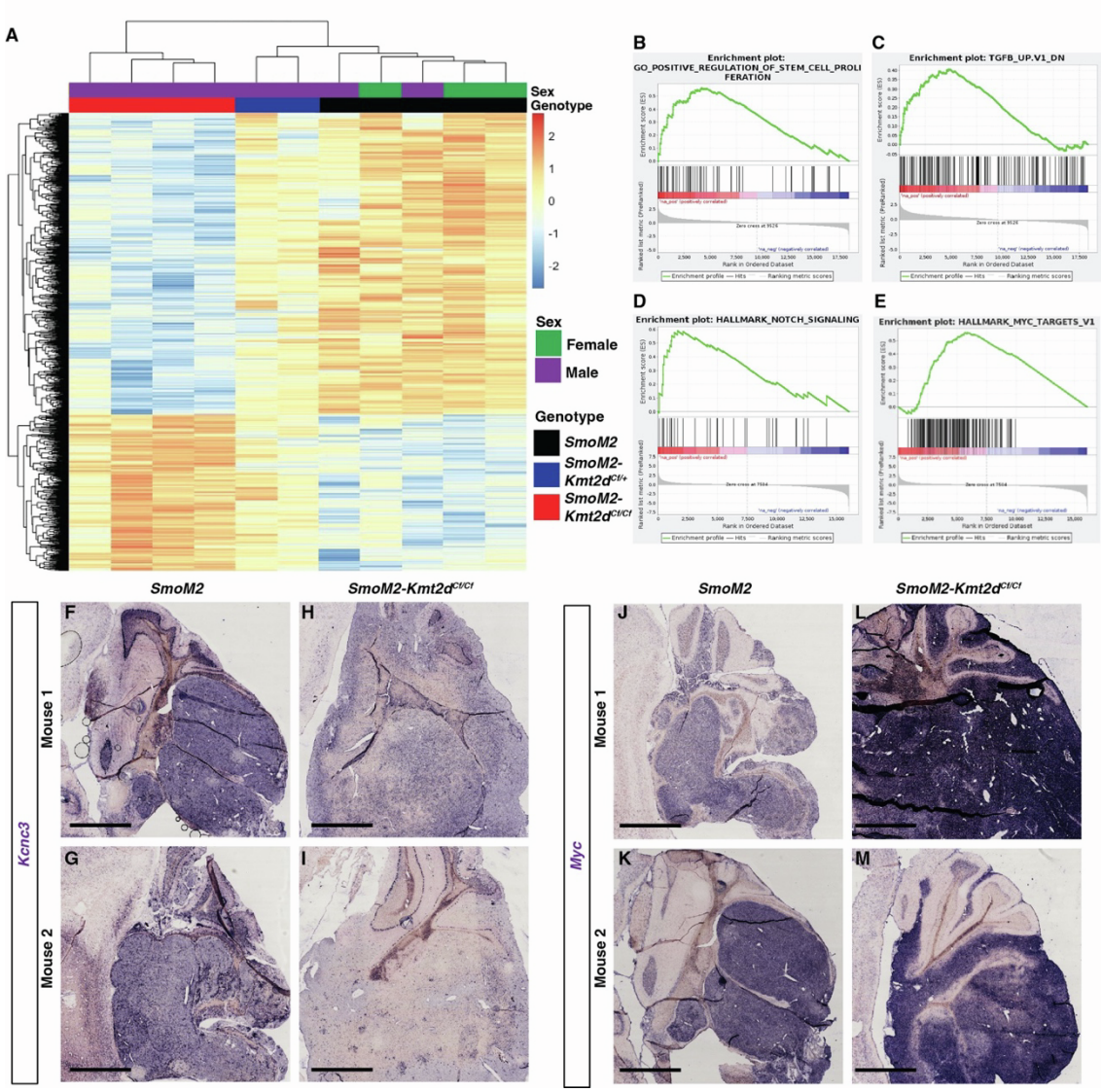

Figure S3: Transcriptomic analyses and validation of RNA-seq data in *SmoM2* tumors reveals upregulated tumor pathways and decreased neural differentiation upon *Kmt2d*^{Cf} mutation. Related to Figure 4.

(A) Heatmap showing unsupervised clustering (p <= 0.05; fold change >= 1.5) of normalized bulk RNA-seq data of primary SHH-MBs from *SmoM2* (n=5), *SmoM2-Kmt2d*$^{Cf/+}$ (n=2) and *SmoM2-Kmt2d*$^{Cf/Cf}$ (n=4) tumors. See also Table S2.

(B-E) Gene set enrichment analysis for genes upregulated in *SmoM2-Kmt2d*$^{Cf/Cf}$ tumors compared to *SmoM2* indicating upregulation of genes associated with stem cell proliferation (B), TGFβ pathway (C), Notch pathway (D), and MYC signaling (E).

(F-M) RNA *in situ* staining showing downregulation of neural differentiation gene *Kcnc3* (F-I) and upregulation of oncogene *Myc* (J-M) in *SmoM2-Kmt2d*$^{Cf/Cf}$ primary tumors compared to *SmoM2* (Scale bar = 500μm).

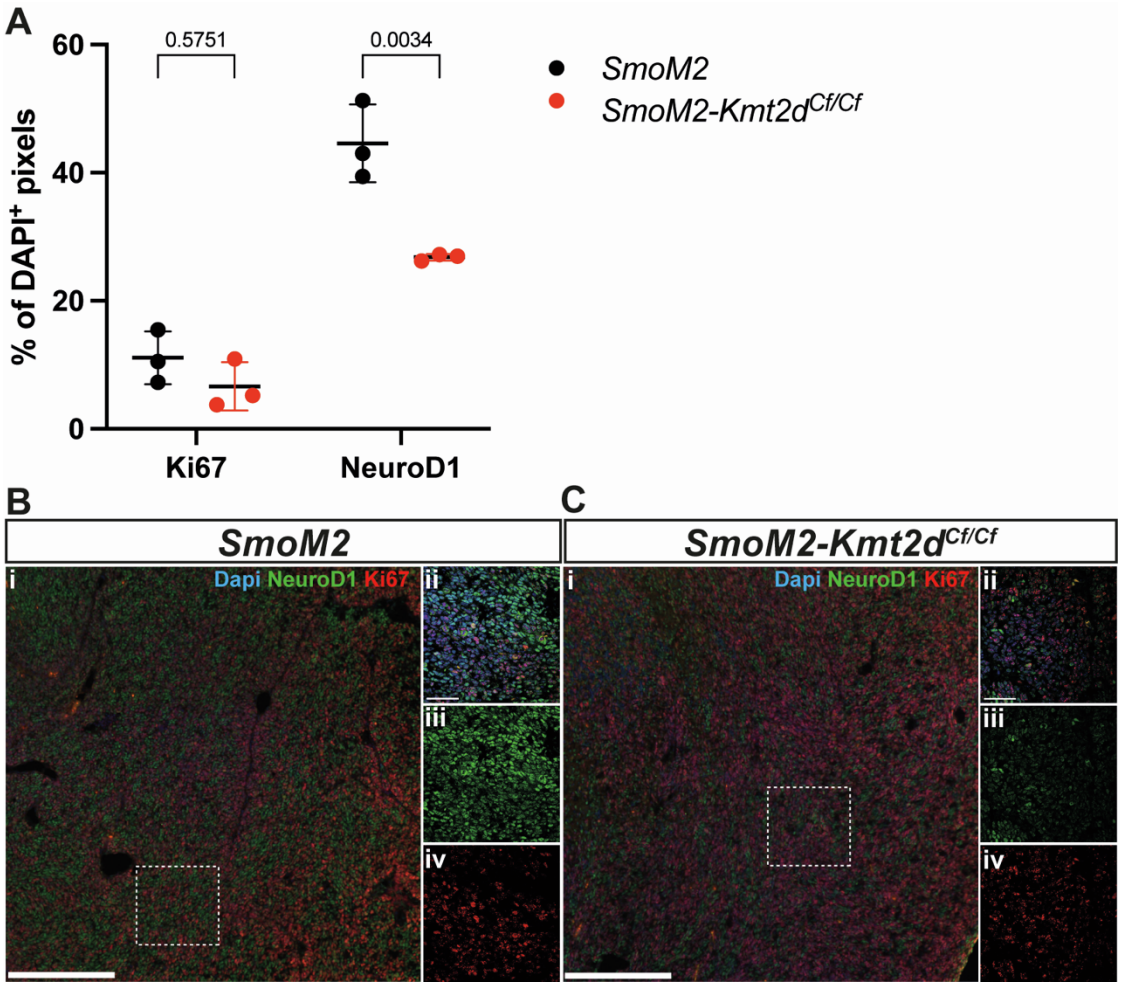

Figure S4: Loss of *Kmt2d* in SHH-MB leads to reduced expression of neural differentiation gene without altering proliferation. Related to Figure 4.

(A) Quantification of the percentage of Ki67+/Dapi+ or NeuroD1+/DAPI+ pixels of totla DAPI+ pixels.

(B - C) Immunostaining of tumor sections from *SmoM2* (B) and *SmoM2-Kmt2*$^{Cf/Cf}$ (C) mice at end stage for Ki67 (red) and NeuroD1 (green) expression. Dapi in blue was used to label DNA in cell nuclei. (ii-iv) Low (i) and high magnification images, showing triple staining (i-ii) or NeuroD1 (iii) and Ki67 (iv) single immunostaining. Approximate areas in confocal high magnification images are indicated by the white box in (i).

Statistical significance was determined by using a 2-way ANOVA test. Error bars: S.D. Scale bar = 250µm (i) and 50µm (ii-iv).

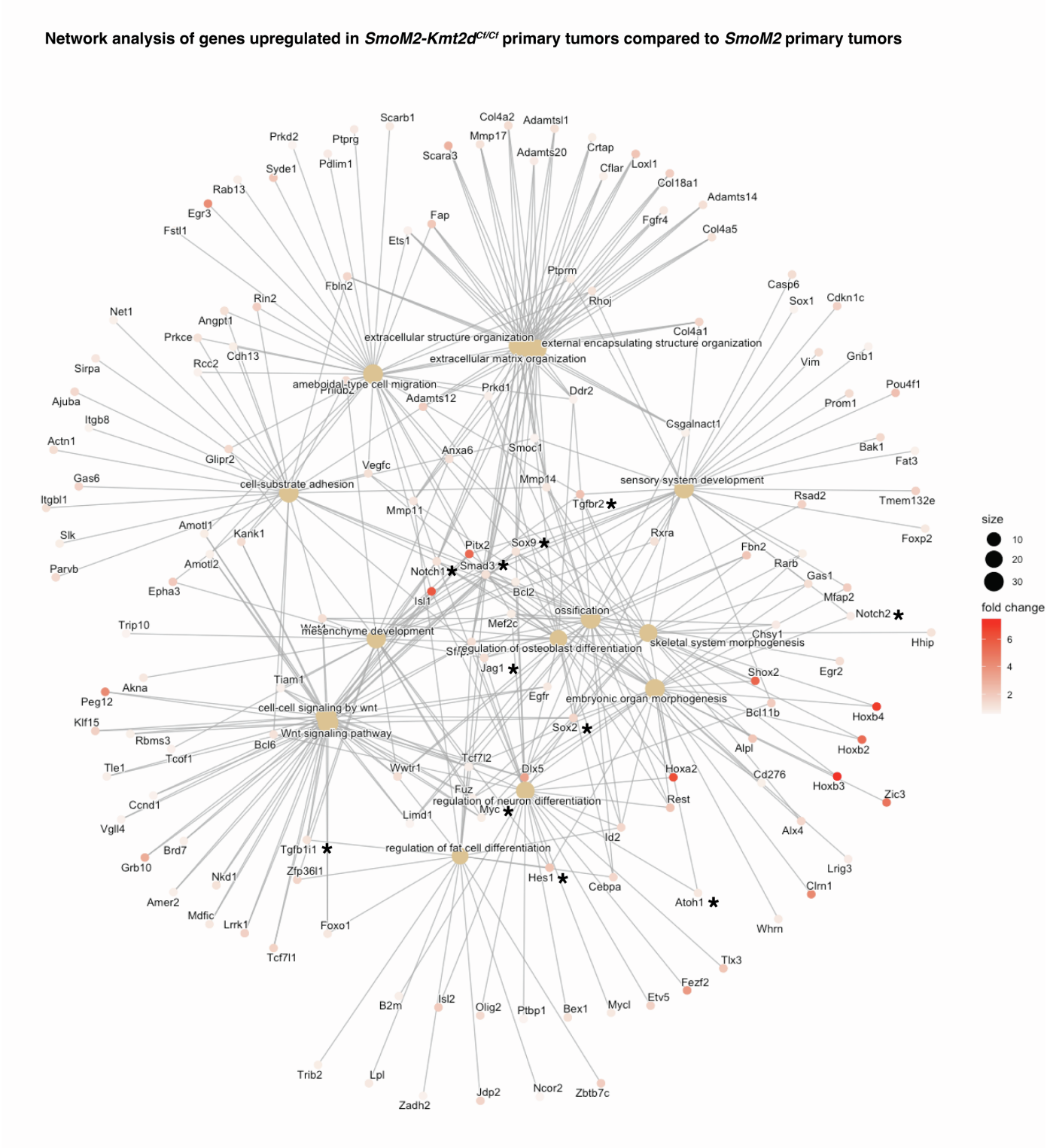

Figure S5: Network analysis of RNA-seq data reveals upregulation of TGFβ and Notch pathway genes and *Myc*, *Atoh1* and *Sox2/9* in primary *SmoM2-Kmt2d*$^{Cf/Cf}$ tumors compared to *SmoM2*. Related to Figure 4.

Network analysis of bulk RNA-seq showing genes and pathways upregulated in primary *SmoM2-Kmt2d*$^{Cf/Cf}$ tumors compared to *SmoM2* (p <= 0.05; FC >= 1.5). Stars indicate genes associated with the TGFβ and Notch pathways and early progenitor populations.

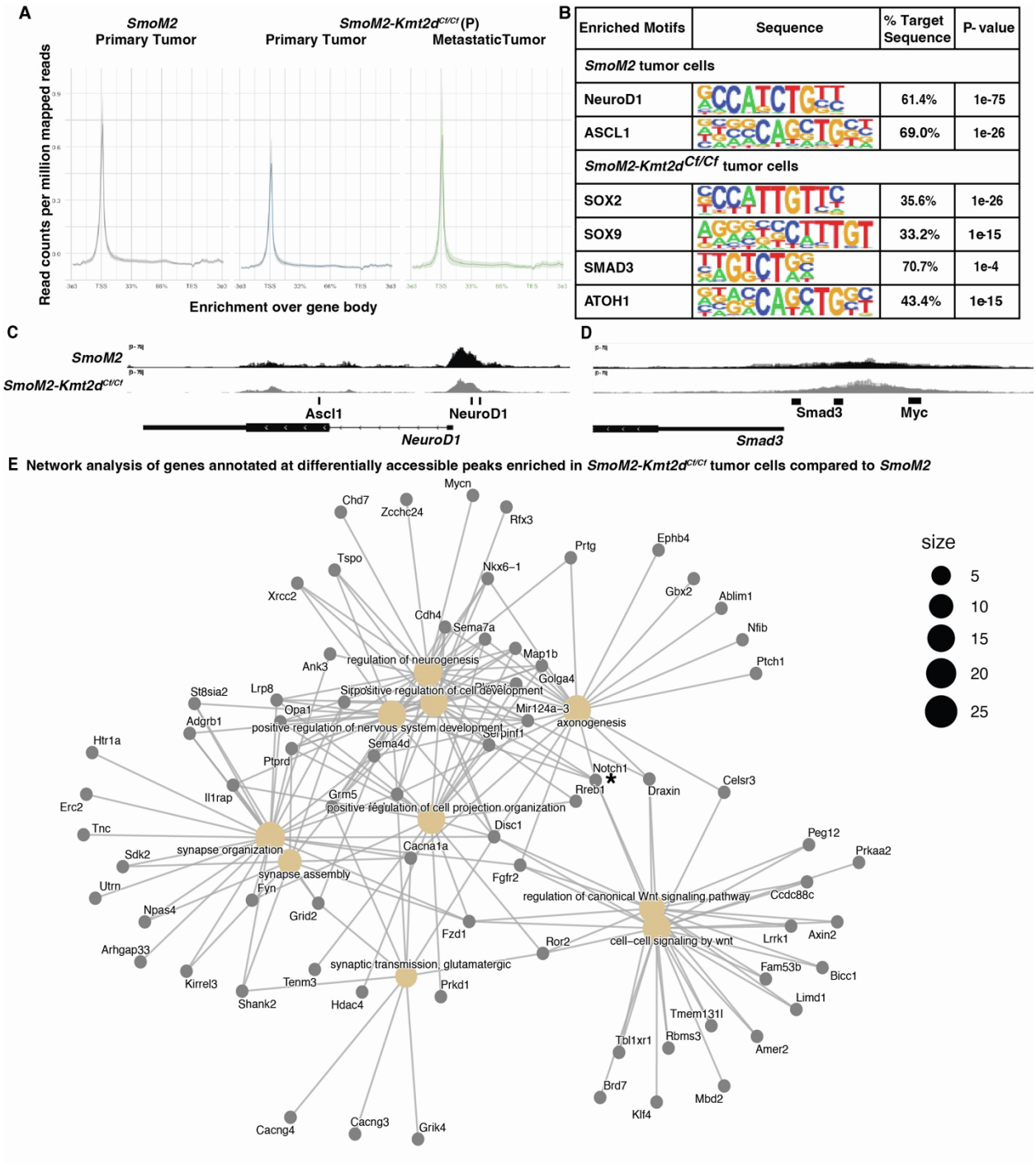

Figure S6: Chromatin accessibility analyses of *SmoM2* and *SmoM2-Kmt2d*$^{Cf/Cf}$ tumors reveals similar changes to RNA-seq, Related to Figure 4, 5.

(A) QC assessment of ATAC-seq data showing signal to noise ratio of *SmoM2* primary and *SmoM2-Kmt2d*$^{Cf/Cf}$ primary and metastatic tumors.

(B) Sequence logos for highly enriched motif sequences in *SmoM2* or *SmoM2-Kmt2d*$^{Cf/Cf}$ tumors.

(C, D) Examples of motifs enriched in *SmoM2* (C) or *SmoM2-Kmt2d*$^{Cf/Cf}$ (D) tumors.

(E) Network analysis of genes annotated at differentially accessible peaks enriched in *SmoM2-Kmt2d*$^{Cf/Cf}$ tumors compared to *SmoM2* shows Notch signaling as a central node for several pathways. Star indicates Notch1 signaling.

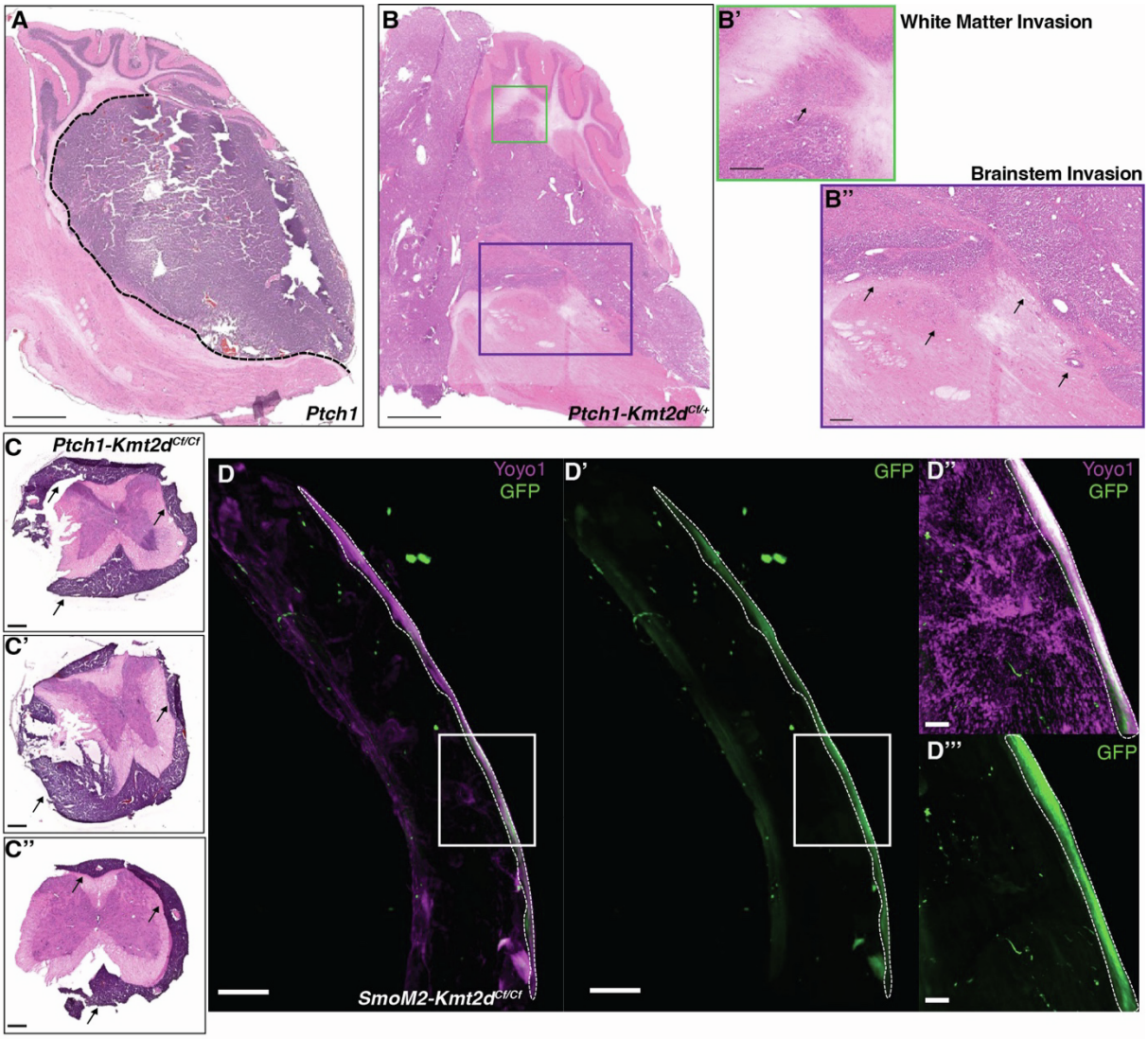

Figure S7: Loss of *Kmt2d* promotes local cell invasion and spinal cord metastasis in the *SmoM2* and *Ptch1* mouse tumor models. Related to Figure 6.

(A-B'') Representative images of sagittal sections from endstage *Ptch1* and *Ptch1-Kmt2d*$^{Cf/+}$ H&E-stained tumors without tumor cell invasion into the WM and the BS (A) and with invasion (B). High magnification images showing invasion into the WM (B') and the BS (B'') in the areas indicated by the green and purple boxes, respectively in B. Arrows indicate areas of tumor cell invasion. A-B: Scale bar = 1mm. B'-B'': Scale bar = 200μm.

(C-C'') Representative spinal cord sections stained with H&E from a *Ptch1-Kmt2d*$^{Cf/Cf}$ animal from anterior to posterior regions. Scale bar = 200μm). Arrows indicate some regions with tumors.

(D-D''') Light sheet coronal images of a cleared spinal cord from a *SmoM2-Kmt2d*$^{Cf/Cf}$ animal stained with a nuclear dye, Yoyo1 (purple) and GFP (green) for tumor cells. High magnification overlay of Yoyo1 and GFP staining (D'') or single channel GFP staining (D''') in the area indicated by the white box in D-D'. D, D': Scale bars = 500μm; D'', D''': Scale bar =100um.

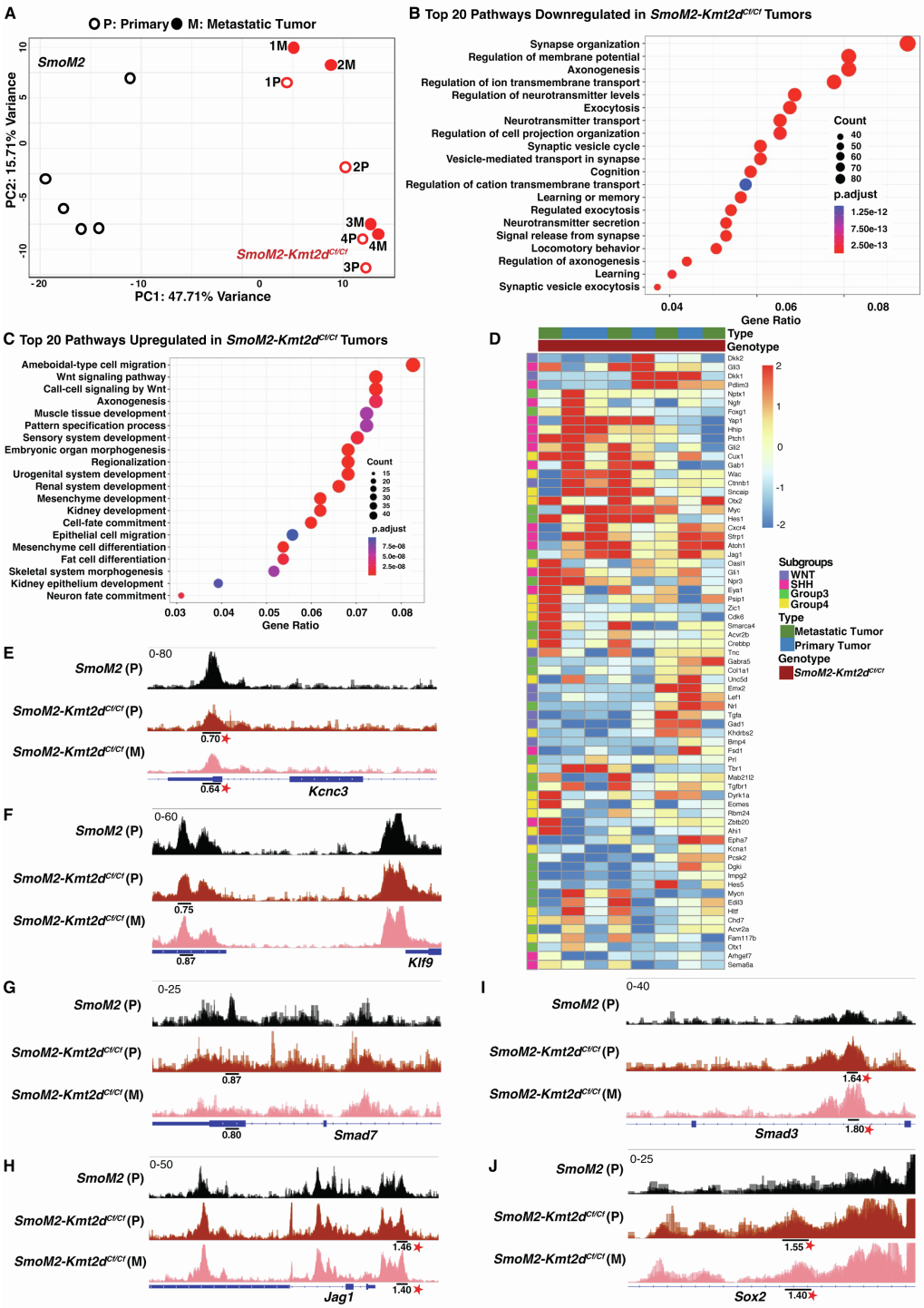

Figure S8: Primary and metastatic *SmoM2-Kmt2d*$^{Cf/Cf}$ tumors down regulate neural differentiation genes and upregulate genes associated aggressive cancer. Related to Figure 7.

(A) PCA analysis of RNA-seq data of *SmoM2-Kmt2d*$^{Cf/Cf}$ primary and metastatic tumors (red circles), and *SmoM2* primary tumors (black circles), open circles are primary tumors.

(B, C) GO term pathway analysis of RNA-seq data shows the genes downregulated (B) and upregulated (C) in *SmoM2-Kmt2d*$^{Cf/Cf}$ primary and metastatic tumors compared to *SmoM2* primary tumors.

(D) Heatmap rendition of MB subgroup-specific genes in *SmoM2-Kmt2d*$^{Cf/Cf}$ primary and metastatic tumors.

(E-H) ATAC-seq analysis showing a chromatin accessibility decrease in a gene associated with neural differentiation (*Kcnc3)* (n=5) (E), and the pathway repressors *Klf9* (F) and *Smad7* (G) and increase in a Notch pathway gene (H), TGFβ pathway gene (I), and early progenitor state gene (J) in *SmoM2-Kmt2d*$^{Cf/Cf}$ primary (n=12) and metastatic (n=6) tumors compared to *SmoM2* primary tumors (n=5). Fold changes with a padj <= 0.1 are indicated with a star.

Table S1: Samples for RNA-seq and ATAC-seq analysis, Related to Figures 4, 5, 7.

Genotype	*SmoM2*						
Age (days)	70	69	76	85	113	53	53
Symptomatic	Yes	No	No	No	No	No	No
ATAC-Seq (P)	Yes	Yes	Yes	Yes	Yes	Yes	Yes
RNA-Seq (P)	No	No	Yes	Yes	Yes	Yes	Yes
Genotype	*SmoM2-Kmt2d*$^{Cf/+}$						
Age (days)	55	62	49	65			
Symptomatic	Yes	No	No	No			
ATAC-Seq (P)	No	No	No	No			
RNA-Seq (P)	No	No	Yes	Yes			
Genotype	*SmoM2-Kmt2d*$^{Cf/Cf}$						
Age (days)	50	57	40	41	40	44	
Symptomatic	Yes	Yes	Yes	Yes	Yes	Yes	
ATAC-Seq (P)	Yes	Yes	Yes	Yes	Yes	Yes	
RNA-Seq (P)	No	No	Yes	Yes	Yes	Yes	
ATAC-Seq (M)	Yes	Yes	Yes	Yes	Yes	Yes	
RNA-Seq (M)	No	No	Yes	Yes	Yes	Yes	

RNA-seq was performed on 1 primary tumor (P) from the left or right hemisphere of animals from all three genotypes and the metastatic spinal cord tumor (M) from the same *Smom2-Kmt2d*$^{Cf/+}$ and *Smom2-Kmt2d*$^{Cf/Cf}$ animals.
ATAC-seq was performed on 1 primary tumor from *SmoM2*, *SmoM2-Kmt2d*$^{Cf/+}$ and *SmoM2-Kmt2d*$^{Cf/Cf}$ animals and the metastatic tumors from the same *SmoM2-Kmt2d*$^{Cf/Cf}$ animals.
P: Primary Tumor; M: Metastatic Tumor